

Validation of Micelle Formation of Proteins and Determination of Their Critical Micelle Concentrations by Measuring Synchronous Light Scattering Signals Using a Common Spectrofluorometer

Hua Wen Zhao,^{1,2} Cheng Zhi Huang,^{*1} and Yuan Fang Li¹

¹College of Chemistry and Chemical Engineering, Southwest University, Chongqing 400715, P. R. China

²Department of Chemistry, Third Military Medical University, Chongqing 400038, P. R. China

(Received January 26, 2006; CL-060114; E-mail: chengzhi@swu.edu.cn)

Micellization of proteins was validated and a method was developed to determine their critical micelle concentration (CMC) values by measuring synchronous light scattering (SYLS) signals using a common spectrofluorometer.

The critical micelle concentration (CMC) represents a fundamental micellar quantity to study the self-aggregation of amphiphilic molecules in solution. The CMC value of an amphiphilic molecule decides the industrial usefulness and biological activity of detergents as well as some other interesting surfactant features like solute-solvent and solute-solute interactions.¹ Thus, to obtain precise value of the CMC is of specially scientific interest. In theory, proteins are amphiphilic molecules consisting of hydrophilic amido, carboxy, and hydrophobic alkyl, whose structure resembles surfactants, so it should be resemblant to some extent to micelle formation. Interactions of proteins and cationic-anionic surfactants have been studied extensively for decades due to their importance in many food industry, pharmaceutical industry, and analytical biochemistry.^{2,3} However, there has been no reports about CMC of protein to our knowledge.

Resonance light scattering (RLS) technique is a newly developed tool by simultaneously scanning the excitation and emission monochromator of a common spectrofluorometer to measure the light scattering singnals.^{4,5} It could provide important information on molecular structure, size, shape, charge distribution, state of combination, and so on, and it has found wide applications in the designation of bio-assemblies and aggregation species since enhanced RLS signals could be measured when the wavelength of the excitation beam is close to the molecular absorption region.⁶⁻⁸ With the same detection mode of signals, by scanning the synchronous light scattering (SYLS) signals through the spectrofluorometer, we found that the SYLS signals of anion and cation surfactants at the characteristic wavelengths take great changes corresponding to their CMC-values using sodium dodecyl sulphate (SDS) and cetyltrimethylammonium bromide (CTMAB) as examples. In analogous way, proteins, such as bovine serum albumin (BSA) and human serum albumin (HSA), display SYLS signals characterized around 316.0–318.0 nm, which take great changes at some concentration with increasing their concentrations, indicating that BSA and HSA are in the state of micelle formation, and thus the CMC values of proteins could be determined with this SYLS signals. These data are identical to the measurements of fluorescence polarization and anisotropy, dynamic light scattering (DLS), and light scattering imaging (LSI).

The SYLS spectrum and intensity were measured with a Hitachi F-4500 spectrofluorometer (Tokyo, Japan) by synchronously scanning with $\lambda_{\text{ex}} = \lambda_{\text{em}}$. As Figure 1 shows, SDS (twice

purified by ethanol prior use) has its own SYLS spectra depending on its concentration over the wavelength range 250.0–650.0 nm, and a characteristic peak could be observed near 320 nm with wide spectra band ranging from 280 to 500 nm. The maximal SYLS intensity is not linear with SDS concentration (see the inserted curve in Figure 1). When SDS concentration is lower than $5.0 \times 10^{-3} \text{ mol L}^{-1}$, the SYLS signals get increased with concentrations because of an increase of the number of scattering particles. However, when SDS concentration is higher than $5.0 \times 10^{-3} \text{ mol L}^{-1}$, the SYLS signals get rapidly decrease at the beginning and then increase gradually, thus an inflexion point of the SYLS intensity in Figure 1 appears at the SDS concentration of $8.8 \times 10^{-3} \text{ mol L}^{-1}$, which is in good agreement with the CMC values of $8.3 \times 10^{-3} \text{ mol L}^{-1}$, determined by conductance method in this study, and $8.1 \times 10^{-3} \text{ mol L}^{-1}$ of other reports.⁹ It was found also that CTMAB has an inflexion point of the SYLS intensity (see Supporting Information), and the concentration of CTMAB is $1.0 \times 10^{-3} \text{ mol L}^{-1}$, which is in good agreement with the CMC values of $9.2 \times 10^{-4} \text{ mol L}^{-1}$.⁹ Thus, we could draw the conclusion that the inflexion points in $I_{\text{SYLS}}-c$ curve indicate the formation of micelle and could be used for CMC detection.

HSA and BSA solution has their SYLS signals over the wavelength range 220–650 nm depending on its concentrations, and characteristic peak could be observed at 318.0 and 316.6 nm, respectively. Figure 2 shows the dependence of the SYLS intensity on HSA and BSA concentration, which is similar to SDS and CTMAB solution, and an inflexion point of the SYLS intensity appears at the concentration value of HSA is $7.69 \times 10^{-3} \text{ mg mL}^{-1}$ in aqueous solution and $8.99 \times 10^{-3} \text{ mg mL}^{-1}$ in

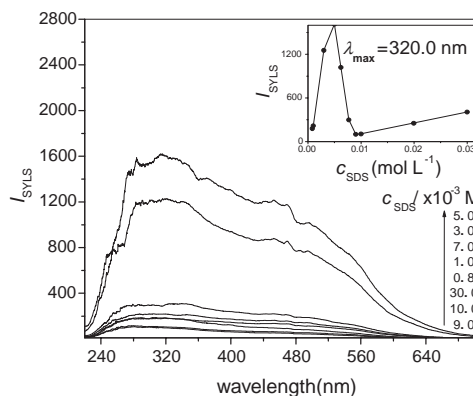


Figure 1. The SYLS spectra of SDS aqueous solution near the CMC. Instrumental conditions: Slit, 10.0 nm; PMT voltage, 400 V. The inserted is the SYLS intensity at 320.0 nm (I_{SYLS}) of SDS aqueous solution as a function of SDS concentration at 25 °C.

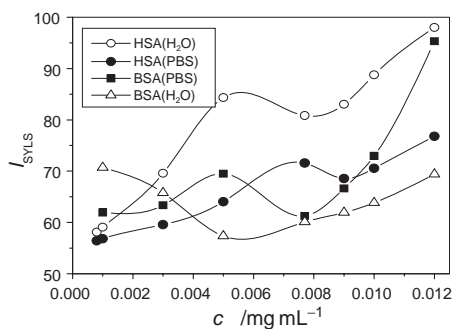


Figure 2. Dependence of the maximal SYLS intensity on BSA and HSA concentration. HSA aqueous solution (\circ), HSA in PBS solution (\bullet), BSA aqueous solution (\triangle), BSA in PBS solution (\blacksquare). HSA: $\lambda_{\max} = 318.0$ nm. BSA: $\lambda_{\max} = 316.6$ nm. Instrumental conditions: Slit: 10.0 nm, PMT voltage: 400 V.

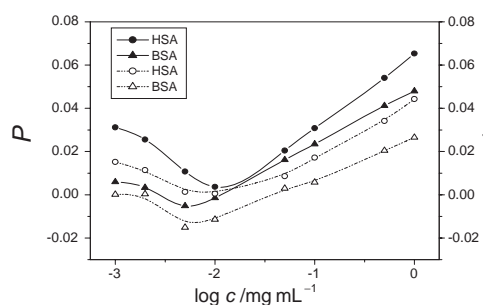


Figure 3. Dependence of fluorescence polarization (solid) and anisotropy (dotted) on BSA and HSA concentration. $\lambda_{\text{ex}} = 280.0$ nm, $\lambda_{\text{em}} = 360.0$ nm, and $\lambda_{\text{em}} = 343.0$ nm for HSA and BSA, respectively. Conditions: Slit, 10.0 nm. PMT voltage, 400 V. Temperature: 25 °C. Fluorescence polarization (P) values and anisotropy (r) values are calculated using the intensities (I) of emitted light polarized either parallel (\parallel) or perpendicular (\perp) to the direction of the electric vector of the polarized exciting light, as indicated in the equation: $P = (I_{\parallel} - I_{\perp}) / (I_{\parallel} + I_{\perp})$, $r = (I_{\parallel} - I_{\perp}) / (I_{\parallel} + 2I_{\perp})$.

PBS solution, while that of BSA is 5.24×10^{-3} mg mL $^{-1}$ in aqueous solution and 7.17×10^{-3} mg mL $^{-1}$ in PBS solution. As proteins are amphiphilic molecules consisting of hydrophilic amido, carboxy, and hydrophobic alkyl, whose structure resembles surfactants, so we suppose that the inflexion point in $I_{\text{SYLS}}-c$ curve indicates that the CMC values of proteins.

We could validate this protein micelle formation by fluorescence polarization and anisotropy, light scattering image (LSI) measurements, and dynamic light scattering (DLS). Figure 3 shows that both HSA and BSA solutions have the lowest fluorescence polarization and anisotropy near 0.01 mg mL $^{-1}$. The state of the lowest fluorescence polarization indicates that the molecule has the lowest volume and the biggest movement speed, showing the formation of small micelle.¹⁰

By introducing an argon ion laser beam to excite the species of BSA solution, we could observe the images of the BSA solution to the excitation beam due to the strong SYLS signals.¹¹ Using a cooled CCD, the LSIs in situ could be caught. Figure 4 displays two-dimensional LSIs of BSA in different concentration near CMC values. There were only a few bright points displayed in the images obtained from 0.01 mg mL $^{-1}$ BSA solution (Figure 4b), however, there are large numbers of the bright

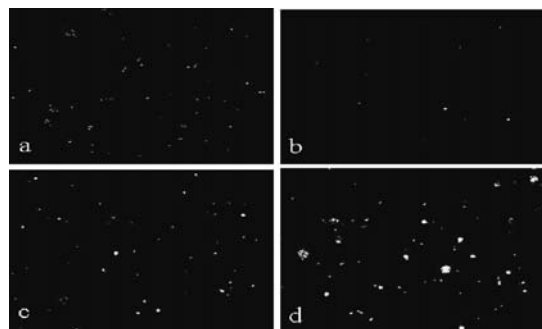


Figure 4. Two-dimensional LSI images of BSA. Concentrations of BSA from figures a to b (mg mL $^{-1}$): 1.0×10^{-3} , 1.0×10^{-2} , 5.0×10^{-2} , and 0.1. The subframe area is 400×300 pixels; and it is about 0.0108 cm 2 by using 1 pixel 3.0×10^{-4} cm when using $4 \times$ objective. Laser power: 0.5 mw.

points displayed in the BSA solution higher or lower than 0.01 mg mL $^{-1}$ (Figures 4a, 4c, and 4d). The bright points disappeared in Figure 4b because of the formation of small micelle, which is too small to engender the light scattering signal. When BSA concentration exceeds 0.01 mg mL $^{-1}$, a large amount of micelle yields, and the size of micelle get enlarged markedly, exhibiting strong LSI signals (Figures 4c and 4d).

DLS measurements, made using a N5 submicron particles size analyzer (Beckman coulter, America), show that the mean size (indicating the hydrodynamic radius R_h) and the relative deviation of DLS data are smallest near the 0.01 mg mL $^{-1}$ (see supporting information), which is much consistent with that detected by SYLS technique, LSI and fluorescence polarization, showing that the formation of micelle particle.

In summary, the state of protein forming micelle has been found by determining the SYLS intensity of protein solutions, and it has been validated by the measurements of fluorescence polarization and anisotropy, light scattering images, and DLS. In addition, our experiments showed that determination of CMC values of proteins by conventional conductance method seems incapable because of large conductance of buffer solution but too small conductance of protein solution in pure water. On the other hand, the present SYLS technique is a simple and economical one to determine protein CMC value.

Financial supports from the NSFC of China (Nos. 20425517 and 30570465) and the Municipal Science and Technology Committee of Chongqing are acknowledged.

References

1. N. B. Li, H. Q. Luo, S. P. Liu, *Spectrochim. Acta, Part A* **2004**, 60, 1811.
2. M. N. Jones, *Chem. Soc. Rev.* **1992**, 21, 127.
3. A. Valstar, M. Almgren, W. Brown, M. Vasilescu, *Langmuir* **2000**, 16, 922.
4. R. F. Pasternack, C. Bustamante, P. J. Collings, A. Giannetto, E. J. Gibbs, *J. Am. Chem. Soc.* **1993**, 115, 5393.
5. R. F. Pasternack, P. J. Collings, *Science* **1995**, 269, 935.
6. C. Z. Huang, K. A. Li, S. Y. Tong, *Anal. Chem.* **1997**, 69, 514.
7. K. Kano, K. Fukuda, H. Wakami, R. Nishiyabu, R. F. Pasternack, *J. Am. Chem. Soc.* **2000**, 122, 7494.
8. R. F. Pasternack, E. J. Gibbs, D. Bruzewicz, D. Stewart, K. S. Engstrom, *J. Am. Chem. Soc.* **2002**, 124, 3533.
9. K. Tajima, M. Muramatsu, T. Sasaki, *Bull. Chem. Soc. Jpn.* **1970**, 43, 1991.
10. K. Nielsen, M. Lin, D. Gall, M. Jolley, *Methods* **2000**, 22, 71.
11. C. Z. Huang, Y. Liu, Y. H. Wang, H. P. Guo, *Anal. Biochem.* **2003**, 321, 236.